



Iranian Research Organization
for Science and Technology
(IROST)

Advances
Environmental
Technology



Journal home page: <https://aet.irost.ir>

Dispersion modeling of SO₂, NO₂, and CO emitted from the Sahand thermal power plant using AERMOD software

Mahdi Saghafi*, Ali Hajiabdollahi Mamaghani

Department of Mechanical Engineering, Faculty of Engineering, University of Bonab, Bonab, Iran.

ARTICLE INFO

Document Type:
Research Paper

Article history:
Received 02 February 2025
Received in revised form
03 January 2026
Accepted 03 February 2026

Keywords:
AERMOD
Carbon monoxide
Nitrogen dioxide
Sahand power plant
Sulfur dioxide

ABSTRACT

In this research, the dispersion of gaseous pollutants emitted from the Sahand thermal power plant was simulated using AERMOD software to determine the concentrations of sulfur dioxide, nitrogen dioxide, and carbon monoxide in the surrounding area. AERMOD was used to analyze the concentration patterns of these pollutants within a 35.9 km² domain, covering the cities of Bonab, Ajabshir, and Khoshehmehr, along with their nearby villages. For this purpose, two years of meteorological data, along with geographical information and emission source characteristics, were utilized to estimate pollutant concentrations over averaging periods of 1 hour, 3 hours, 24 hours, and annual averages. Comparison of the modeled results with the limits defined in the environmental standards indicates that the maximum concentrations of nitrogen oxide and carbon monoxide in residential areas are within the permissible limits. However, the highest concentration of sulfur dioxide exceeds the limits in some villages, suggesting a potential health risk for residents.

1. Introduction

The modeling of atmospheric pollutant emissions is a fundamental tool for investigating air quality conditions and the dispersion patterns of harmful substances that threaten both human health and the environment. The complete elimination of industrial pollutants remains an unattainable goal given current technological capabilities.

Therefore, it is imperative to identify the specific substances emitted by power plants and assess their environmental impacts, as failure to do so could lead to serious health risks for citizens.

Consequently, comprehensive research and analysis are essential to mitigate the dangers posed by these pollutants. Globally, 6% of annual deaths are attributed to premature mortality caused by air pollution. In Iran, this figure is even higher, around 10% [1]. Estimating the dispersion of air pollutants from various sources is the first step towards controlling environmental conditions and improving public health. Experimental measurements of air pollution provide valuable information about pollutants and their concentrations within a given region [2]. However, such measurements are limited to the specific

*Corresponding author Tel.: +98 4161811621

E-mail: msaghafi@ubonab.ac.ir

DOI: 10.22104/aet.2026.7387.2052

COPYRIGHTS: ©2026 Advances in Environmental Technology (AET). This article is an open access article distributed under the terms and conditions of the Creative Commons Attribution 4.0 International (CC BY 4.0) (<https://creativecommons.org/licenses/by/4.0/>)

locations and times, and cannot be generalized to other areas, particularly in regions with complex terrain. Furthermore, determining the maximum pollutant concentrations in a given area requires repeated measurements at multiple locations and times, which can be time-consuming and costly.

Nevertheless, it is possible to estimate pollutant concentrations at unmeasured locations or future times, even with limited data, by applying data-driven methods such as artificial neural networks [3] and support vector machines. These estimating methods are subject to uncertainties arising from various factors that influence pollutant distribution, making them less suitable for use in environmental monitoring programs. In contrast, model-based techniques can offer a more comprehensive understanding of pollution dispersion by describing the complex interactions between pollutant emissions, meteorological parameters, and regional topography. Mathematical models of pollutant dispersion can therefore provide more detailed guidance for implementing control measures and evaluating the effectiveness of different strategies to reduce pollutant concentrations.

The Gaussian model is one of the oldest methods for modeling the dispersion of atmospheric pollutants and remains the most widely used and accepted method for calculating the pollutant concentrations at specific points, compared to other methods such as the Eulerian and Lagrangian models [4, 5]. Gaussian models are valuable tools for simulating point sources of pollutant emissions, such as those from power plants and refinery chimneys. Also, it is possible to develop relationships that allow the application of Gaussian models to line sources (e.g., roads) and area sources (e.g., fires in pastures and forests). To conduct an air pollution dispersion analysis using a Gaussian model, it is essential to gather information on pollutant sources, including the mass emission rate of the materials, the velocity and temperature of exhaust gases, and the emission height. Additionally, meteorological data, such as wind speed and direction, ambient air temperature, and other parameters used to determine the atmosphere stability class, must also be collected [4].

American Meteorological Society-Environmental Protection Agency Regulatory Model (AERMOD) is a steady-state Gaussian plume-based emission modeling software that performs transport calculations within a wind field [6]. In addition to modeling point sources, it can also be used to model linear pollutant sources generated by vehicular movement on roads and streets [7-14]. AERMOD includes two preprocessors, AERMET for meteorological data processing and AERMAP for terrain and land-use information, to prepare the input data required for pollutant dispersion modeling based on the Gaussian model. AERMOD has been widely used to model the dispersion of conventional pollutants emitted from various industrial activities, including power plants [15-19], refineries [20-27], steel industries [28], and cement factories [29]. AERMOD has also been applied widely in specialized studies, such as modeling of sulfur dioxide emissions from airports near coastlines [30], sulfur compounds emissions from sewage reservoirs [31-33], odor emissions from livestock farms [34] and landfills [35], benzene emissions from gas stations [29], particulate matter emissions from cotton ginning factories [36] and open-cast copper mines [37], gaseous pollutant emissions of from ships [38, 39], dispersion of SARS-CoV-2-laden particulate matters [40], heavy metal emissions from coke plants [41], radon gas emissions from uranium mines [42, 43] and the release of radioactive materials from nuclear power plants [44]. In all these cases, AERMOD has provided reliable results. Thermal power plants that burn fossil fuels near urban areas are among the primary sources of air pollution emissions, continuously affecting the environment [15]. The combustion of fossil fuels releases air pollutants, such as carbon oxides (CO_x), nitrogen oxides (NO_x), sulfur oxides (SO_x), and particulate matter (PM), into the atmosphere [45-48]. To determine the impact of each power plant on the surrounding region, it is necessary to perform precise modeling of pollutant emissions using the geographical and meteorological data of that area. In this research, a point source was used in AERMOD to model pollutant emissions from the Sahand thermal power plant. The cities of Bonab, Ajabshir, and Khoshehmehr, along with their surrounding villages, are located near the Sahand

thermal power plant. This closeness highlights the importance of accurately modeling the pollutant emissions from this power plant to assess its environmental impacts. In this paper, the concentrations of sulfur dioxide, nitrogen dioxide, and carbon monoxide in the vicinity of the Sahand thermal power plant were determined using AERMOD to model pollutant dispersion. Comparing the concentrations of these pollutants with the permissible limits defined in relevant standards reveals the environmental impact of the power plant on the surrounding area. The novelty of this research lies in conducting a realistic and detailed analysis characterized by the following features:

- Development of a detailed AERMOD model based on the specific geometric data of the Sahand thermal power plant chimney, actual pollutant emission rate measurements, two years of meteorological data from the nearest synoptic weather station, and terrain elevation data that accounts for surrounding mountains and the plant's cooling towers.
- Simultaneous dispersion modeling of the three major pollutants (sulfur dioxide, nitrogen dioxide, and carbon monoxide) over four time scales (1-hour, 3-hour, 24-hour, and the annual average).
- Evaluation of the calculated pollutant concentrations in both cities and villages within a 50 km radius of the plant, and comparison of the results with the corresponding limits specified in Iranian national standards and WHO guidelines.

2. Materials and methods

2.1. Dispersion modeling with AERMOD

In this study, the AERMOD software, which is based on the steady-state Gaussian plume model for

short-range dispersion (less than 50 km), was used to investigate the dispersion patterns of pollutants emitted from the chimney of the Sahand thermal power plant. The power plant is located in the southwest of East Azerbaijan province, in northwestern Iran (Figure 1).

The geographical coordinates of the Sahand power plant are 589,609 meters east and 4,142,366 meters north, with an elevation of 1,292 meters above sea level. According to the Mercator global coordinate system, it falls within the S38 zone.

The power plant consists of two units operating on a steam Rankine cycle, each with a nominal production capacity of 325 MW.

Table 1 shows the dimensions of the power plant chimney and the properties of the released gases. The release rate of pollutant gases (in grams per second) was calculated using measured mass concentration (in grams per cubic meter) and the total volumetric flow rate.

The total volumetric flow rate of exhaust gases was obtained by multiplying the measured velocity of exhaust gases by the cross-sectional area of the chimney outlet. The properties of the exhaust gases were measured by the Iranian Department of Environment (DOE) using a Testo combustion gas analyzer under ambient conditions of 10°C and 86.35 kPa. During the measurement period, Unit 1 of the power plant operated on liquid fuel to produce 260 MW of electricity, while Unit 2 was undergoing scheduled maintenance.

In this study, the Sahand thermal power plant was modeled as a point emission source within a square domain with a side length of 35.9 km.

The computational domain includes 129,600 receptors arranged orthogonally in a 360×360 grid, with a spacing of 100 meters between receptors.

Table 1. Characteristics of the power plant chimney and the emission rate of released gases.

Chimney height (m)	Chimney diameter (m)	Exhaust gas temperature (°C)	Exhaust gas velocity (m/s)	Release rate of SO ₂ (g/s)	Release rate of NO ₂ (g/s)	Release rate of CO (g/s)
200	4.5	151.5	27.84	1460.3	86.33	2.08



Fig. 1. Location of the Sahand thermal power plant.

To model pollutant emissions, it is essential to consider not only the characteristics of the emission source but also the ground effects and meteorological conditions of the study area. The required meteorological parameters include wind speed and direction, dry-bulb temperature, humidity, pressure, cloud cover, and rainfall. As mentioned earlier, meteorological data processing in AERMOD is performed using the AERMET preprocessor. AERMET uses meteorological data and land surface characteristics to calculate intermediate parameters such as Albedo, Bowen ratio, and surface roughness for each receptor. The average values of Albedo, Bowen ratio, and surface roughness calculated for the study area over two years were 0.18, 0.75, and 0.065, respectively. AERMET then computes atmospheric boundary layer parameters, including the friction velocity, Monin-Obukhov length, convective velocity scale, temperature scale, mixing height, and surface heat flux. Boundary layer parameters are subsequently used to generate vertical profiles of wind speed, lateral and vertical turbulence fluctuations (σ_v , σ_w), potential temperature gradient ($d\theta/dz$), and potential temperature (θ) within the AERMOD model [49]. Also, the AERMAP preprocessor uses WGS84 elevation data to evaluate the effects of terrain height and determine the spatial relationship between the pollutant emission source (i.e., power plant chimney location) and each receptor.

The following assumptions were adopted in this modeling process: temporal independence of emissions, absence of interactions among different emission sources, and no reduction in pollution concentration due to chemical interactions, absorption, or sedimentation. Also, the calculated pollutant concentrations for each receptor represent the maximum values over the averaging periods of 1-hour, 3-hour, 24-hour, and annual average.

In this research, meteorological data from the Bonab synoptic meteorological station, provided by the Iranian Meteorological Organization, were used for the period 2020/12/21 to 2022/12/22. These data were collected at 3-hour intervals and include wind speed and direction, temperature, humidity, pressure, cloud cover, and rainfall for all days. The processed results from the AERMET preprocessor indicate that the prevailing wind direction during these two years was predominantly from east to west (Figure 2).

3. Results and discussion

The results of the dispersion modeling for sulfur dioxide (SO_2), nitrogen dioxide (NO_2), and carbon monoxide (CO) pollutants are presented in Figures 3 to 5, respectively. These figures illustrate the highest concentrations of pollutants recorded at all receptors located in the vicinity of the Sahand thermal power plant during the two-year simulation period. For each pollutant, the maximum concentration values were calculated

using four averaging periods, i.e., 1-hour, 3-hour, 24-hour, and annual average, which are denoted as (a), (b), (c), and (d) in the figures, respectively.

According to the Iranian ambient air quality standard [50], the permissible limits for the maximum concentrations of sulfur dioxide, carbon monoxide, and nitrogen dioxide gases in various averaging periods are as follows:

- Sulfur dioxide: $196 \mu\text{g.m}^{-3}$ in a 1-hour period and $395 \mu\text{g.m}^{-3}$ in a 24-hour period,
- Nitrogen dioxide: $200 \mu\text{g.m}^{-3}$ in a 1-hour period and $100 \mu\text{g.m}^{-3}$ as an annual average,

- Carbon monoxide: 40mg.m^{-3} in a 1-hour period and 10mg.m^{-3} in an 8-hour period.

On the other hand, the World Health Organization recommends the following criteria for these pollutants [51]:

- Sulfur dioxide: 40mg.m^{-3} in a 24-hour period,
- Nitrogen dioxide: $200 \mu\text{g.m}^{-3}$ in a 1-hour period, $25 \mu\text{g.m}^{-3}$ in a 24-hour period, and $10 \mu\text{g.m}^{-3}$ as an annual average,
- Carbon monoxide: 35mg.m^{-3} in a 1-hour period, 10mg.m^{-3} in an 8-hour period, and 4mg.m^{-3} in a 24-hour period.

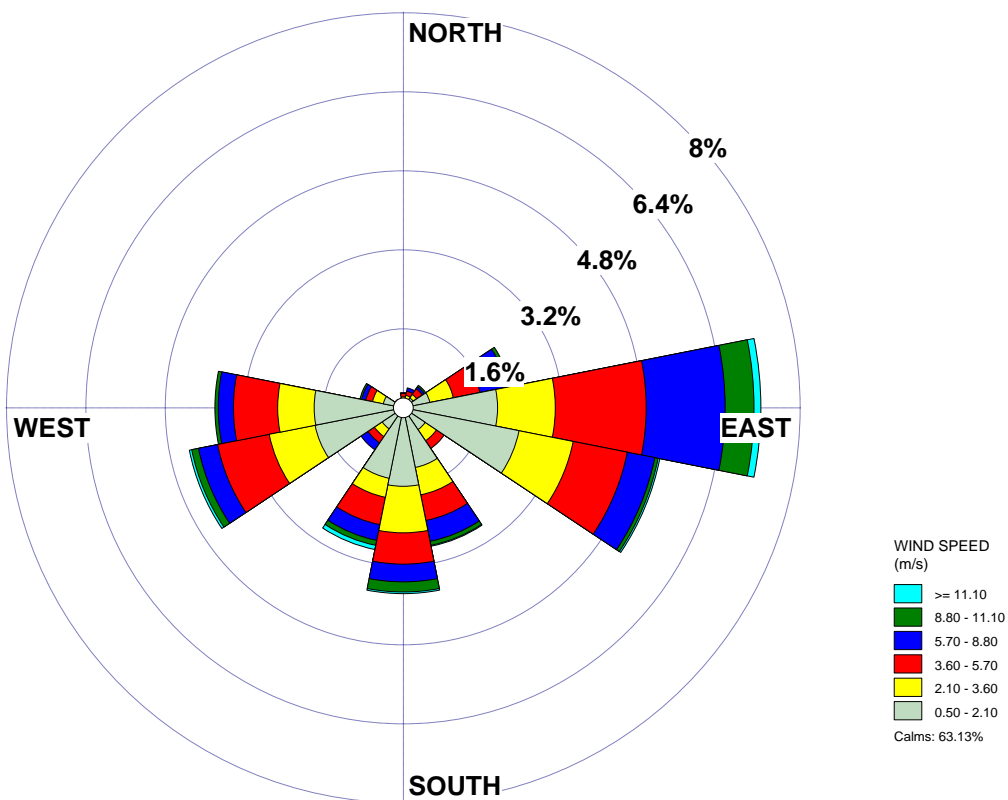


Fig. 2. Wind rose diagram of the study area.

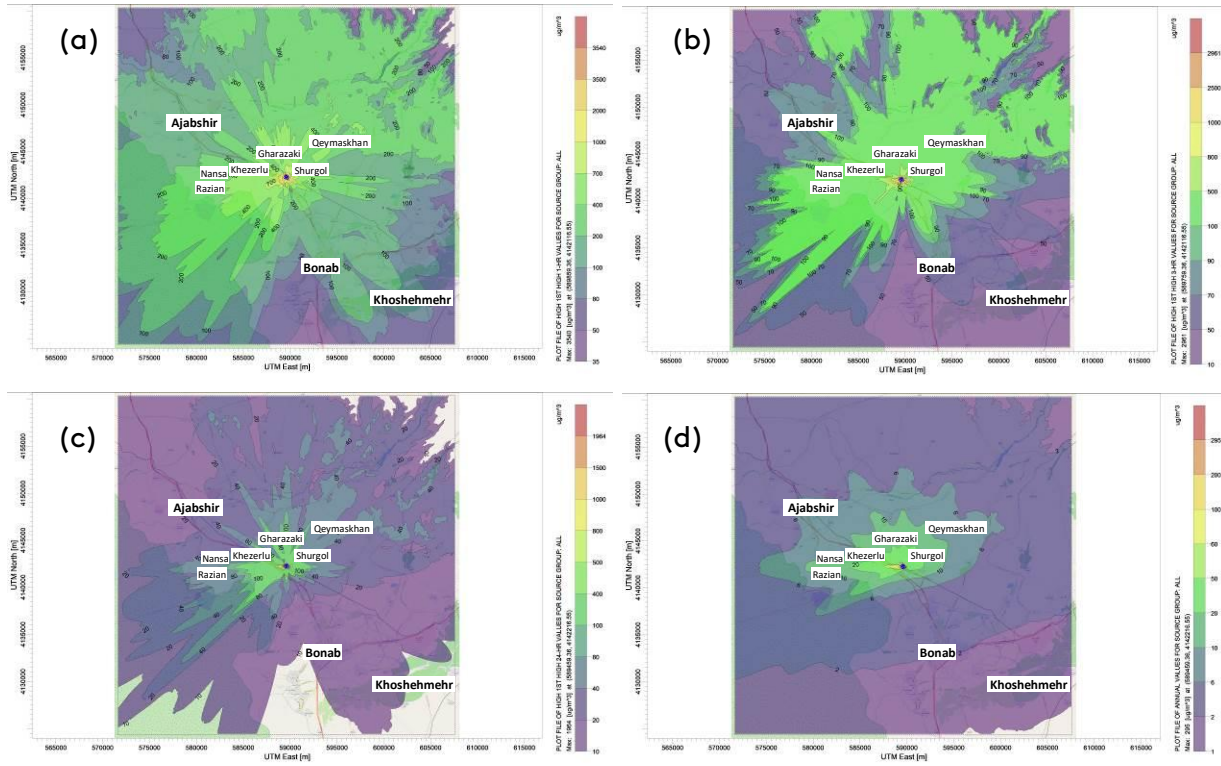


Fig. 3. Highest SO₂ concentration in different periods: (a) 1-hour, (b) 3-hour, (c) 24-hour, and (d) annual average.

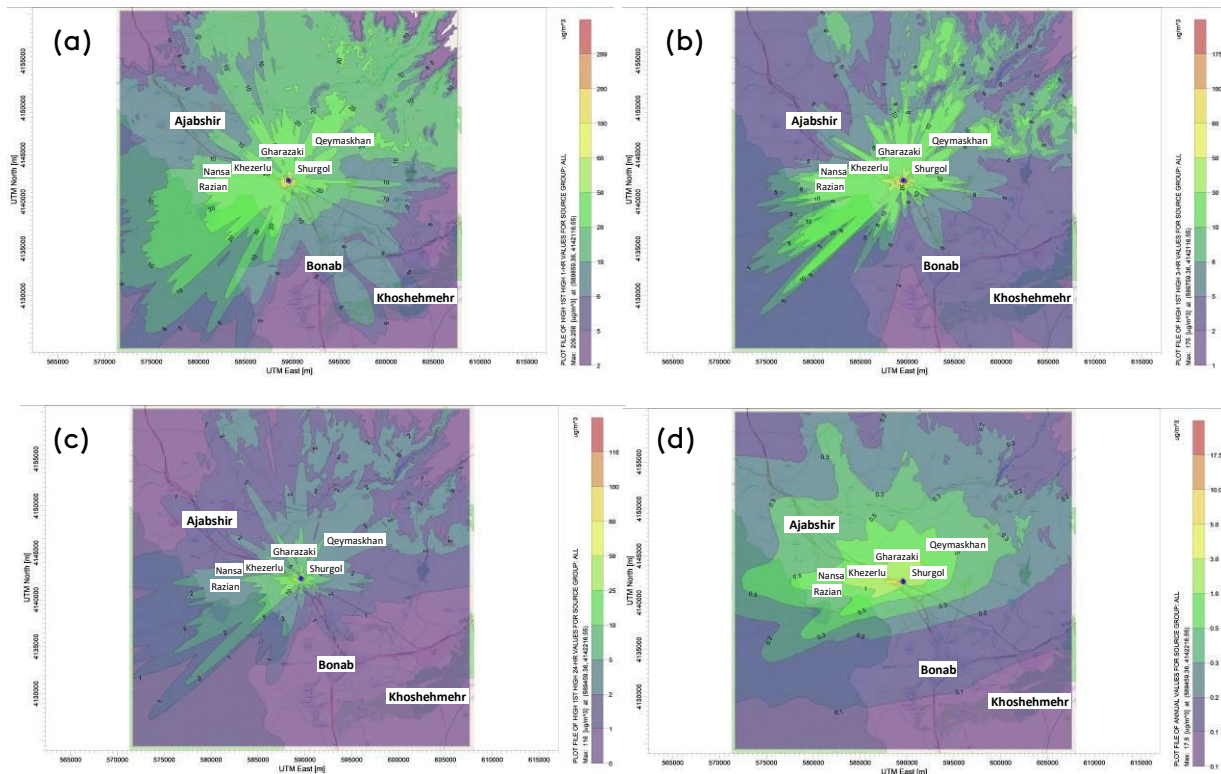


Fig. 4. Highest NO₂ concentration in different periods: (a) 1-hour, (b) 3-hour, (c) 24-hour, and (d) annual average.

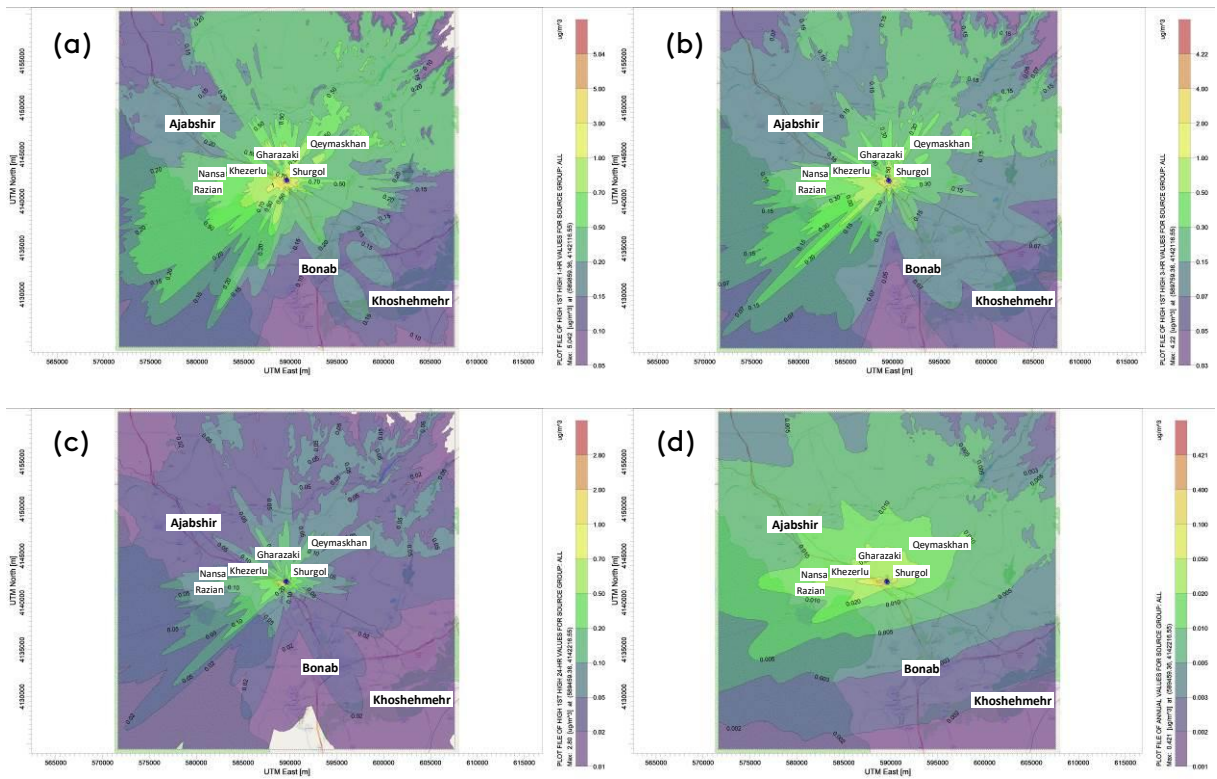


Fig. 5. Highest CO concentration in different periods: (a) 1-hour, (b) 3-hour, (c) 24-hour, and (d) annual average.

According to the modeling results, the highest 1-hour concentration of sulfur dioxide is $3539.63 \mu\text{g}\cdot\text{m}^{-3}$ (Figure 6a), the highest 1-hour concentration of nitrogen dioxide is $209.25 \mu\text{g}\cdot\text{m}^{-3}$ (Figure 6b), and the highest 1-hour concentration of carbon monoxide is $5.04 \mu\text{g}\cdot\text{m}^{-3}$ (Figure 6c). All three maximum concentration points are located within the Sahand power plant site, approximately 100–139 meters from the emission source (chimney). The presence of large structures near the chimney, such as the cooling towers, induces turbulence, leading to downwash effects that increase pollutant concentrations near the ground. According to these results during a 1-hour averaging period, the maximum concentration of sulfur dioxide is approximately 18 times higher than the Iranian standard, the maximum concentration of nitrogen dioxide is about 5% higher than both the Iranian and WHO limits, and the maximum concentration of carbon monoxide is 7000 times lower than the permissible limit of the WHO and 8000 times lower than the limit of Iranian standard.

The following presents and compares the calculated concentrations of pollutants emitted from the Sahand thermal power plant for densely populated residential areas adjacent to the plant with the criteria specified in both the Iranian and the WHO standards.

1-hour averaging period:

The maximum 1-hour concentration of sulfur dioxide (Figure 3a) was below $196 \mu\text{g}\cdot\text{m}^{-3}$ (the Iranian 1-hour limit) in all nearby cities of the Sahand power plant (Bonab, Ajabshir, and Khoshehmehr). However, in several nearby villages, the sulfur dioxide concentration exceeded this limit, reaching up to twice the limit in Qeymaskhan, Khezerlu, Nansa, and Nabrin, and up to three times the limit in Shurgol and Gharazaki. According to the 1-hour distributions of nitrogen dioxide and carbon monoxide in Figures 4a and 5a, respectively, the maximum concentrations of both pollutants outside the power plant were below the permissible limits set by both the Iranian and WHO standards.

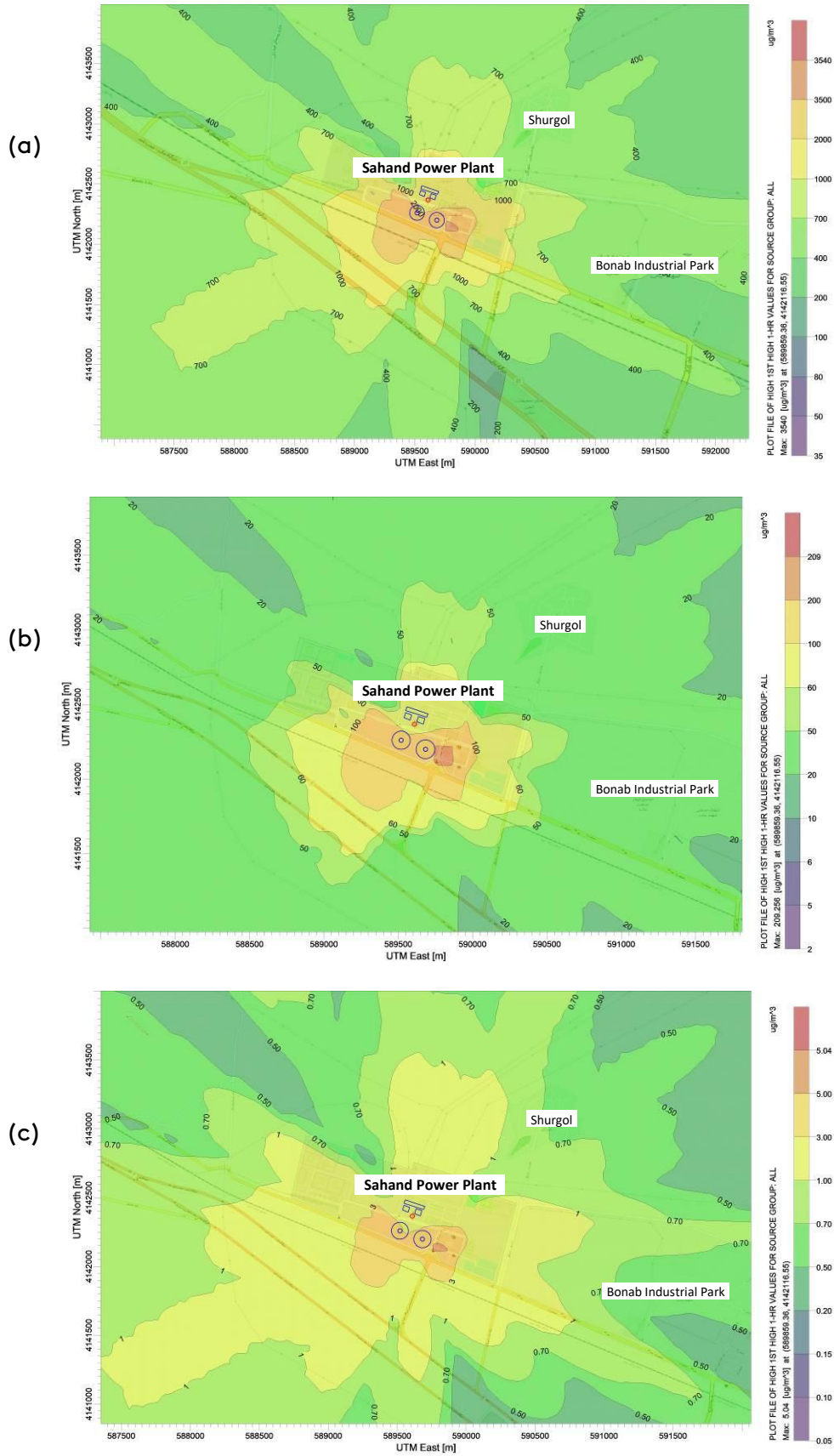


Fig. 6. The location of the highest 1-hour pollutant concentrations: (a) sulfur dioxide, (b) nitrogen dioxide, and (c) carbon monoxide.

In the cities of Bonab, Khoshehmehr, and Ajabshir, the concentrations of nitrogen dioxide ranged from 5 to 10 $\mu\text{g}\cdot\text{m}^{-3}$, which is approximately 20 times lower than the permissible limit. Additionally, the concentrations of carbon monoxide ranged from 0.3 to 0.5 $\mu\text{g}\cdot\text{m}^{-3}$ in the above-mentioned cities, significantly below the corresponding thresholds.

3-hour averaging period:

Figures 3b, 4b, and 5b illustrate the maximum concentrations of sulfur dioxide, nitrogen dioxide, and carbon monoxide over a 3-hour averaging period, respectively. The highest concentration of sulfur dioxide was below 100 $\mu\text{g}\cdot\text{m}^{-3}$ in the cities of Bonab, Khoshehmehr, and Ajabshir, but increased to 500 $\mu\text{g}\cdot\text{m}^{-3}$ in the Shurgol village. Also, the highest concentration of nitrogen dioxide ranged from 2 to 6 $\mu\text{g}\cdot\text{m}^{-3}$ in the nearby cities of the Sahand power plant. Finally, the maximum carbon monoxide concentration was 4.22 $\mu\text{g}\cdot\text{m}^{-3}$ across the entire modeling domain.

24-hour averaging period:

Figure 3c shows that the maximum 24-hour averaging concentration of sulfur dioxide remained below 40 $\mu\text{g}\cdot\text{m}^{-3}$ (the WHO limit) in all the cities surrounding the power plant. However, in several villages (Shurgol, Gharazaki, Khezerlu, Nansa, Nabrin, and Razian), it rose to about 180 $\mu\text{g}\cdot\text{m}^{-3}$, which was still lower than the Iranian limit of 395 $\mu\text{g}\cdot\text{m}^{-3}$. The maximum concentration of nitrogen dioxide (Figure 4c) in all cities and villages around the power plant was below 25 $\mu\text{g}\cdot\text{m}^{-3}$, satisfying the WHO standard. Additionally, the highest 24-hour concentration of carbon monoxide (Figure 5c) was 2.8 $\mu\text{g}\cdot\text{m}^{-3}$, well below the WHO limit.

Annual average:

The annual average concentration of sulfur dioxide (Figure 3d) in the cities of Bonab and Khoshehmehr was below 3 $\mu\text{g}\cdot\text{m}^{-3}$, while in Ajabshir, it ranged between 5 and 8 $\mu\text{g}\cdot\text{m}^{-3}$. In Shurgol village, the sulfur dioxide concentration increased to 35 $\mu\text{g}\cdot\text{m}^{-3}$. The annual average concentration of nitrogen dioxide (Figure 4d) was below 10 $\mu\text{g}\cdot\text{m}^{-3}$ (the WHO limit) in all nearby cities, though it reached up to 40 $\mu\text{g}\cdot\text{m}^{-3}$ in some villages, still below the Iranian standard limit. Furthermore, the highest concentration of carbon monoxide in all the areas

surrounding the Sahand power plant was 0.4 $\mu\text{g}\cdot\text{m}^{-3}$, far below the permissible levels in both standards.

4. Conclusion

In this research, the dispersion of pollutant gases emitted from the Sahand power plant chimney was modeled using AERMOD software. The maximum concentrations of the sulfur dioxide, nitrogen dioxide, and carbon monoxide in the different averaging periods (1-hour, 3-hour, 24-hour, and annual average) were calculated for 129600 receptors arranged orthogonally with a spacing of 100 m. The modeling domain covered the cities of Bonab, Ajabshir, and Khoshehmehr, along with their surrounding villages. Comparison of the simulated results with the environmental standards of Iran and the WHO revealed the following findings:

- Sulfur dioxide concentrations in all surrounding cities were below the limits set by both the Iranian and WHO standards for the 1-hour and 24-hour averaging periods. However, in several nearby villages, the highest 1-hour concentration of sulfur dioxide exceeded the Iranian limit, reaching up to three times the standard value. In the 24-hour averaging period, the sulfur dioxide concentrations in all villages were below the Iranian limit, although in some villages close to the power plant, they reached 4.5 times the WHO limit.
- Nitrogen dioxide concentrations were below both the Iranian and WHO standards for the 1-hour averaging period and below the WHO limit for the 24-hour averaging period. The annual average concentration of this pollutant in the cities surrounding the plant remained within the WHO limit. However, it reached up to four times the WHO limit in some villages, remaining below the Iranian limit.
- Carbon monoxide concentrations across the entire modeling domain were well below both Iranian and WHO limits in 1-hour and 24-hour averaging periods.

Overall, the findings indicate that among the pollutants emitted from the chimney of the Sahand thermal power plant, sulfur dioxide poses the greatest potential health risk to nearby residents,

particularly in the surrounding villages. To reduce sulfur dioxide concentration in nearby villages, the emission of this pollutant can be mitigated by switching from liquid fuel to natural gas or by using a mixture of liquid fuel and natural gas. This approach would decrease the amount of sulfur dioxide released and consequently its ambient concentration.

Furthermore, it is possible to optimize fuel type management based on meteorological conditions and prevailing wind directions, thereby minimizing the impact of emissions on nearby residential areas.

For future studies, it is recommended to extend the modeling to include pollutant emissions from other industrial sources located in the Bonab industrial park, which lies adjacent to the Sahand power plant.

This approach would enable a comprehensive assessment of the cumulative air pollution impacts in the region.

Acknowledgements

The authors would like to thank the Iranian Meteorological Organization (IRIMO), the Iranian Department of Environment (DOE), and the Sahand Power Plant for providing the requisite data.

Author's contribution

Mahdi Saghafi: conceptualization, literature research, methodology, visualization, supervision, writing, reviewing, and editing. Ali Hajiabdollahi Mamaghani: conceptualization, data curation, modeling, visualization, writing. All the authors reviewed the manuscript before submission.

Conflict of interest

No potential conflict of interest was reported by the authors.

Data availability

Not Applicable.

Funding

Self-funded.

References

- [1] Abdi, A., Abessi, O., & Khavasi, E. (2022). Numerical Modeling for transport and distribution of carbon monoxide plume in indoor spaces and stagnant environment. *Journal of Research in Environmental Health*, 8(3), 233-248.
<https://doi.org/10.22038/jreh.2022.63262.1478>
- [2] Aleahmad, M., Karbassi, A., Davami, A. H., & Jalilzadeh Yengejeh, R. (2022). A feasibility study of using Mahshahr city's meteorological and air quality data to evaluate air pollution. *Journal of Research in Environmental Health*, 8(2), 148-159.
<https://doi.org/10.22038/jreh.2022.63933.1492>
- [3] Asaei-Moamam, Z.-S., Safi-Esfahani, F., Mirjalili, S., Mohammadpour, R., & Nadimi-Shahraki, M.-H. (2023). Air quality particulate-pollution prediction applying GAN network and the neural Turing machine. *Applied Soft Computing*, 110723.
<https://doi.org/10.1016/j.asoc.2023.110723>
- [4] Snoun, H., Krichen, M., & Chérif, H. (2023). A comprehensive review of Gaussian atmospheric dispersion models: current usage and future perspectives. *Euro-Mediterranean Journal for Environmental Integration*, 8(1), 219-242.
<https://doi.org/10.1007/s41207-023-00354-6>
- [5] Leelőssy, Á., Molnár, F., Izsák, F., Havasi, Á., Lagzi, I., & Mészáros, R. (2014). Dispersion modeling of air pollutants in the atmosphere: a review. *Open Geosciences*, 6(3), 257-278.
<https://doi.org/10.2478/s13533-012-0188-6>
- [6] Cimorelli, A. J., Perry, S. G., Venkatram, A., Weil, J. C., Paine, R. J., Wilson, R. B., . . . Brode, R. W. (2005). AERMOD: A Dispersion Model for Industrial Source Applications. Part I: General Model Formulation and Boundary Layer Characterization. *Journal of Applied Meteorology*, 44(5), 682-693.
<https://doi.org/10.1175/JAM2227.1>
- [7] Francisco, D. M., Heist, D. K., Venkatram, A., Brouwer, L. H., & Perry, S. G. (2022). Observations and parameterization of the effects of barrier height and source-to-barrier distance on concentrations downwind of a roadway. *Atmospheric Pollution Research*, 13(4), 101385.

- <https://doi.org/10.1016/j.apr.2022.101385>
- [8] Munjal, A., Sharma, S., Nema, A. K., & Kota, S. H. (2022). Factors affecting particulate matter levels near highway toll plazas in India. *Transportation Research Part D: Transport and Environment*, 110, 103403. <https://doi.org/10.1016/j.trd.2022.103403>
- [9] Irankunda, E., Török, Z., Mereuță, A., Gasore, J., Kalisa, E., Akimpaye, B., Ozunu, A. (2022). The comparison between in-situ monitored data and modelled results of nitrogen dioxide (NO₂): case-study, road networks of Kigali city, Rwanda. *Heliyon*, 8(12), e12390. <https://doi.org/10.1016/j.heliyon.2022.e12390>
- [10] Mostafavi, S. A., Dadsetan, A., & Safikhani, H. (2022). Particulate material 2.5 change in the city using EURO4 urban buses technology case study: Arak City, Iran. *International Journal of Environmental Science and Technology*, 19(10), 10041-10052. <https://doi.org/10.1007/s13762-022-04205-9>
- [11] Mohd Shafie, S. H. (2024). Application of AERMOD dispersion model for assessment PM₁₀ concentrations from mobile sources in Kuala Lumpur Metropolitan City, Malaysia. *Environmental Monitoring and Assessment*, 196(10), 969. <https://doi.org/10.1007/s10661-024-13088-x>
- [12] Grassi, Y. S., & Díaz, M. F. (2024). Urban air pollution evaluation in downtown streets of a medium-sized Latin American city using AERMOD dispersion model. *Environmental Monitoring and Assessment*, 196(6), 521. <https://doi.org/10.1007/s10661-024-12699-8>
- [13] Alhajeri, N. S., Al-Fadhli, F. M., Aly, A., & Allen, D. T. (2024). Quantifying the impact of urban road traffic on air quality: activity pre-pandemic and during partial and full lockdowns. *Environmental Monitoring and Assessment*, 196(5), 418. <https://doi.org/10.1007/s10661-024-12572-8>
- [14] Singh, S., & Gokhale, S. (2023). Modeling the dispersion of traffic-derived black carbon emissions into hilly terrain. *Environmental Monitoring and Assessment*, 195(8), 958. <https://doi.org/10.1007/s10661-023-11554-6>
- [15] Ghorbani, H., & Talebi, A. F. (2023). Dispersion modeling of NO_x and SO₂ pollutions using AERMOD model (Case study of Shahid Salimi power plant, Neka). *Journal of Environmental Science Studies*, 8(2), 6647-6661. <https://doi.org/10.22034/jess.2023.375831.1919>
- [16] Josimović, B., Todorović, D., Jovović, A., & Manić, B. (2024). Air pollution modeling to support strategic environmental assessment: case study—National Emission Reduction Plan for coal-fired thermal power plants in Serbia. *Environment, Development and Sustainability*, 26(6), 16249-16265. <https://doi.org/10.1007/s10668-023-03186-0>
- [17] Changotra, R., Rajput, H., & Dhir, A. (2020). Comparative Study of Air Pollution Modeling Techniques from Point Source(s) of Thermal Power Plant. *Environmental Modeling & Assessment*, 25(4), 531-543. <https://doi.org/10.1007/s10666-020-09704-y>
- [18] Saghafi, M., & Hajiabdollahi Mamaghani, A. (2024). Modeling the dispersion of pollutant gases from the chimney of the Tabriz thermal power plant with AERMOD software. *Journal of Research in Environmental Health*, 9(4), 374-386. <https://doi.org/10.22038/jreh.2024.23859>
- [19] Kudahi, S. N. (2024). Evaluation of mercury emissions from the first coal-fired power plant in Iran using atmospheric dispersion modeling. *International Journal of Environmental Science and Technology*. <https://doi.org/10.1007/s13762-024-05874-4>
- [20] Mott, A., & Guo, H. (2022). Odour dispersion modelling, impact criteria, and setback distances for an oil refinery plant. *Atmospheric Environment*, 270, 118879. <https://doi.org/10.1016/j.atmosenv.2021.118879>
- [21] Rahimi, R., Mansouri, N., Alsheikh, A. A., & Mirzahoseini, A. (2021). Evaluation of amount, emission factors and concentrations of SO₂, NO₂ and CO in ILAM Gas Refinery. *Journal of Environmental Science and Technology*, 23(3), 71-85. <https://doi.org/10.30495/jest.2020.40777.4503>
- [22] Keykhosravi, S. S., Nejadkoorki, F., & Zamani, S. (2023). Developing a Risk Assessment Model for Respiratory Exposure to Toxic Chemical pollutants in one of gas refineries in South Pars using a Combination of AERMOD and SQRA Methods. *J-Health-Saf-Work*, 13(1), 109-128.

- [23] Hallaji, H., Bohloul, M. R., Peyghambarzadeh, S. M., & Azizi, S. (2023). Measurement of air pollutants concentrations from stacks of petrochemical company and dispersion modeling by AERMOD coupled with WRF model. *International Journal of Environmental Science and Technology*, 20(7), 7217-7236. <https://doi.org/10.1007/s13762-023-04959-w>
- [24] Karimi, S., Asghari, M., Rabie, R., & Emami Niri, M. (2023). Machine learning-based white-box prediction and correlation analysis of air pollutants in proximity to industrial zones. *Process Safety and Environmental Protection*, 178, 1009-1025. <https://doi.org/10.1016/j.psep.2023.08.096>
- [25] Eslamidoost, Z., Samaei, M. R., Hashemi, H., Baghapour, M. A., Arabzadeh, M., Dehghani, S., & Rajabi, S. (2023). Assessment of air quality using AERMOD modeling: a case study in the Middle East. *Environmental Monitoring and Assessment*, 195(11), 1272. <https://doi.org/10.1007/s10661-023-11879-2>
- [26] Saikomol, S., Thepanondh, S., & Laowagul, W. (2019). Emission losses and dispersion of volatile organic compounds from tank farm of petroleum refinery complex. *Journal of Environmental Health Science and Engineering*, 17(2), 561-570. <https://doi.org/10.1007/s40201-019-00370-1>
- [27] Mardani, M., Nowrouzi, M., & Abyar, H. (2025). Assessing the environmental impact of offshore flares in the Persian Gulf: A comprehensive analysis of SO₂ emissions. *Advances in Environmental Technology*, 11(1), 63-74. <https://doi.org/10.22104/aet.2024.6494.1781>
- [28] Hesami Arani, M., Jaafarzadeh, N., Moslemzadeh, M., Rezvani Ghalhari, M., Bagheri Arani, S., & Mohammadzadeh, M. (2021). Dispersion of NO₂ and SO₂ pollutants in the rolling industry with AERMOD model: a case study to assess human health risk. *Journal of Environmental Health Science and Engineering*, 19(2), 1287-1298. <https://doi.org/10.1007/s40201-021-00686-x>
- [29] Hsieh, P. Y., Shearston, J. A., & Hilpert, M. (2021). Benzene emissions from gas station clusters: a new framework for estimating lifetime cancer risk. *Journal of Environmental Health Science and Engineering*, 19(1), 273-283. <https://doi.org/10.1007/s40201-020-00601-w>
- [30] Pandey, G., Venkatram, A., & Arunachalam, S. (2023). Evaluating AERMOD with measurements from a major U.S. airport located on a shoreline. *Atmospheric Environment*, 294, 119506. <https://doi.org/10.1016/j.atmosenv.2022.119506>
- [31] Moreno-Silva, C., Calvo, D. C., Torres, N., Ayala, L., Gaitán, M., González, L., . . . Susa, M. R. (2020). Hydrogen sulphide emissions and dispersion modelling from a wastewater reservoir using flux chamber measurements and AERMOD® simulations. *Atmospheric Environment*, 224, 117263. <https://doi.org/10.1016/j.atmosenv.2020.117263>
- [32] Li, R., Han, Z., Shen, H., Qi, F., & Sun, D. (2021). Volatile sulfur compound emissions and health risk assessment from an A2/O wastewater treatment plant. *Science of The Total Environment*, 794, 148741. <https://doi.org/10.1016/j.scitotenv.2021.148741>
- [33] Luckert, A., Aguado, D., García-Bartual, R., Lafita, C., Montoya, T., & Frank, N. (2023). Odour mapping and air quality analysis of a wastewater treatment plant at a seaside tourist area. *Environmental Monitoring and Assessment*, 195(8), 1013. <https://doi.org/10.1007/s10661-023-11598-8>
- [34] Huang, D., & Guo, H. (2023). Performance of AERMOD for predicting livestock odour dispersion under Canadian Prairies climate and flat terrain. *Biosystems Engineering*, 226, 223-237. <https://doi.org/10.1016/j.biosystemseng.2023.01.015>
- [35] Sonibare, O. O., Adeniran, J. A., & Bello, I. S. (2019). Landfill air and odour emissions from an integrated waste management facility. *Journal of Environmental Health Science and Engineering*, 17(1), 13-28. <https://doi.org/10.1007/s40201-018-00322-1>
- [36] Yang, Z., Evans, M. N., Buser, M. D., Hapeman, C. J., Torrents, A., & Whitelock, D. P. (2023). Improving modeling of low-altitude particulate matter emission and dispersion: A

- cotton gin case study. *Journal of Environmental Sciences*, 133, 8-22.
<https://doi.org/10.1016/j.jes.2022.03.048>
- [37] Khazini, L., Dehkharghanian, M. E., & Vaezihir, A. (2022). Dispersion and modeling discussion of aerosol air pollution caused during mining and processing of open-cast mines. *International Journal of Environmental Science and Technology*, 19(2), 913-924.
<https://doi.org/10.1007/s13762-021-03225-1>
- [38] Mendoza-Lara, O. O., Ortega-Montoya, C. Y., Prieto Hinojosa, A. I., López-Pérez, A. O., & Baldasano, J. M. (2023). An empirical and modelling approach to the evaluation of cruise ships' influence on air quality: The case of La Paz, Mexico. *Science of The Total Environment*, 886, 163855.
<https://doi.org/10.1016/j.scitotenv.2023.163855>
- [39] Ekmekçioğlu, A., Çelebi, U. B., Ünlügençoğlu, K., & Kuzu, S. L. (2024). Effect of the low sulphur regulations of maritime fuels on ambient air quality: a case study in the Bosphorus strait. *International Journal of Environmental Science and Technology*.
<https://doi.org/10.1007/s13762-024-05901-4>
- [40] Rezaali, M., & Fouladi-Fard, R. (2021). Aerosolized SARS-CoV-2 exposure assessment: dispersion modeling with AERMOD. *Journal of Environmental Health Science and Engineering*, 19(1), 285-293.
<https://doi.org/10.1007/s40201-020-00602-9>
- [41] Zeng, W., Wan, X., Gu, G., Lei, M., Yang, J., & Chen, T. (2023). An interpolation method incorporating the pollution diffusion characteristics for soil heavy metals - taking a coke plant as an example. *Science of The Total Environment*, 857, 159698.
<https://doi.org/10.1016/j.scitotenv.2022.159698>
- [42] Zhang, H., Gao, J., Bai, Y., Zhou, L., & Xu, L. (2022). Delimiting radiation protection distance of underground uranium mining and metallurgy facilities: A case study in China. *Heliyon*, 8(12), e12419.
<https://doi.org/10.1016/j.heliyon.2022.e12419>
- [43] Lolila, F., & Mazunga, M. S. (2023). Measurements of natural radioactivity and evaluation of radiation hazard indices in soils around the Manyoni uranium deposit in Tanzania. *Journal of Radiation Research and Applied Sciences*, 16(1), 100524.
<https://doi.org/10.1016/j.jrras.2023.100524>
- [44] Ghaemi far, S., Aghaie, M., Minucmehr, A., & Alahyarizadeh, G. (2019). Evaluation of atmospheric dispersion of radioactive materials in a severe accident of the BNPP based on Gaussian model. *Progress in Nuclear Energy*, 113, 114-127.
<https://doi.org/10.1016/j.pnucene.2019.01.019>
- [45] Ganji, A., Babae, A., & Shayegan, J. (2025). Integrating Biomass into Petrochemical Processes: A Review of Feedstock Options and Conversion Routes. *Advances in Environmental Technology*, 11(4), 460-475.
<https://doi.org/10.22104/aet.2025.7758.2181>
- [46] Mukta, T. A., Hoque, M. M. M., Sarker, M. E., Hossain, M. N., & Biswas, G. K. (2020). Seasonal variations of gaseous air pollutants (SO₂, NO₂, O₃, CO) and particulates (PM_{2.5}, PM₁₀) in Gazipur: an industrial city in Bangladesh. *Advances in Environmental Technology*, 6(4), 195-209.
<https://doi.org/10.22104/aet.2021.4890.1320>
- [47] Nihalani, S., Jariwala, N., & Khembete, A. (2023). Characterisation and source apportionment of atmospheric particulate matter in an industrial cluster of Western India. *Advances in Environmental Technology*, 9(3), 242-257.
<https://doi.org/10.22104/aet.2023.5917.1627>
- [48] Birjandi, N., Ghobadi, M., & Ahmadi, M. (2019). Analysis and zoning of air pollution in urban landscape using different models of spatial analysis (Case study: Tehran). *Advances in Environmental Technology*, 5(3), 185-191.
<https://doi.org/10.22104/aet.2020.4251.1210>
- [49] US-EPA. (2023). *AERMOD Model Formulation*. Research Triangle Park, NC: Office of Air Quality Planning and Standards Air Quality Assessment Division.
- [50] Department of Environment. (2017). Ambient Air Quality Standard. Retrieved 2023/10/21.
- [51] World Health Organization. (2021). *WHO global air quality guidelines: particulate matter*

(PM2.5 and PM10), ozone, nitrogen dioxide, sulfur dioxide and carbon monoxide. Geneva: World Health Organization.

How to cite this paper:



Saghafi, M. & Hajiabdollahi Mamaghani, A. (2026). Dispersion modeling of SO₂, NO₂, and CO emitted from the Sahand thermal power plant using AERMOD software. *Advances in Environmental Technology*, 12(1), 89-102. DOI: 10.22104/aet.2026.7387.2052